

# Measurement of the PPN Parameter $\gamma$ with Radio Signals from the Cassini Spacecraft at X- and Ka-Bands

John D. Anderson, Eunice L. Lau, and Giacomo Giampieri\*  
 Jet Propulsion Laboratory, California Institute of Technology, Pasadena, CA 91109, USA

Radio Doppler data from the Cassini spacecraft during its solar conjunction in June 2002 can be used to measure the bending of light by solar gravitation. In terms of the standard post-Newtonian parameter  $\gamma$ , we find that  $\gamma - 1 = (-1.3 \pm 5.2) \times 10^{-5}$ , in agreement with the theory of General Relativity. This result implies that the parameter  $\omega$  in the Brans-Dicke theory is greater than 9000 at a 95% confidence level.

## 1. INTRODUCTION

The Cassini spacecraft, currently orbiting Saturn, is equipped with multi-frequency radio links dedicated to Radio Science Doppler experiments. During the Cassini Mission's cruise phase between Jupiter and Saturn, two relativity tests were planned, one for the solar conjunction of 2002 (SCE1) and the other for the conjunction of 2003 (SCE2). However, after the success of SCE1, hardware problems with the attitude control system (ACS), in particular the reaction wheels, caused the Cassini Project to cancel SCE2. Data from only the 2002 conjunction are available for a relativity test on the Cassini mission.

In addition to the favorable multi-link tracking, the SCE1 experiment was carried out on reaction wheels for an interval of 30 days, with no thrusting by the ACS for attitude control, thereby minimizing the effects of nongravitational forces on the spacecraft trajectory. Outside of the loss of some Doppler data prior to conjunction, because of temporary problems with a Ka-Band transmitter at the Goldstone station (DSS25) of the Deep Space Network (DSN), the experiment went exactly as planned.

## 2. THEORETICAL BACKGROUND

According to the theory of General Relativity (GRT), a light ray propagating in the Sun's gravitational field is effectively refracted, with the vacuum index of refraction  $n$  augmented by a refractivity inversely proportional to the distance  $r$  from the Sun's center of mass.

The gravitational field causes ray bending towards the Sun's center, one of the classical GRT tests, and in addition, electromagnetic waves are time delayed and frequency shifted[1]. In terms of the Sun's Schwarzschild radius,  $R_g = 2GM_\odot/c^2 = 2.9532$  km, the effective refractivity to first order in  $R_g/R_\odot$  is given by,

$$n = 1 + \frac{1 + \gamma}{2} \frac{R_g}{r}. \quad (1)$$

where  $\gamma$  (exactly unity in GRT) is a post Newtonian parameter (PPN) that measures the amount of space curvature produced by solar gravity[2]. Time-delay tests became feasible in the 1960's with the advent of radar ranging to planets and radio ranging to spacecraft, as pointed out by Shapiro[3]. The excess gravitational time delay  $\Delta t$  can be derived from Eq. 1 for a two-way signal transmitted from Earth (uplink), received by a spacecraft, and transmitted back to Earth (downlink). The result for electromagnetic propagation between point 1 and point 2 in heliocentric coordinates is[4],

$$\Delta t = (1 + \gamma) \frac{R_g}{c} \ln \left( \frac{r_1 + r_2 + r_{12} + \left(\frac{1+\gamma}{2}\right) R_g}{r_1 + r_2 - r_{12} + \left(\frac{1+\gamma}{2}\right) R_g} \right) \quad (2)$$

where  $r_1$  is the heliocentric coordinate distance to point 1,  $r_2$  is the distance to point 2, and  $r_{12}$  is the distance between point 1 and point 2. The term in  $R_g$  inside the natural logarithm results from an integration of the coordinate speed of light ( $v < c$ ) along the curved path between point 1 and point 2. Eq. 2 is the expression actually coded in the software used for our data analysis, JPL's Orbit Determination Program (ODP). Doppler data are represented in the ODP as differenced range by Eq. 2. Before SCE1, radio ranging to Viking Landers on the surface of Mars provided the most accurate measurement of  $\gamma$  ( $1.000 \pm 0.002$ )[5].

## 3. CASSINI RADIO SCIENCE DATA

Ideally, a Doppler experiment generates continuous phase data (cycle count) for several days about conjunction, thereby providing accumulative range-change information to much better accuracy than the ranging data, which is limited by about a seven meter random error. In practice, the Cassini Doppler experiment relies on non continuous Doppler data, with each

---

\*Electronic address: john.d.anderson@jpl.nasa.gov, eunice.lau@jpl.nasa.gov, giacomo.giampieri@jpl.nasa.gov

measurement integrated over an interval  $T_C = 300$  s. The Doppler data is effectively a time series of frequency measurements, averaged over each  $T_C$  interval, but with both small gaps of several minutes and large gaps of about 16 hours or more. Only one station of the DSN, DSS25 at Goldstone California, is equipped with a Ka-Band (34,316 MHz) transmitter, required for full Doppler accuracy, hence continuous data is impossible.

Here we present results for an independent analysis of closed-loop (CL) Doppler data retrieved from the Navigation System at JPL. A separate analysis, using open-loop (OL) data from JPL's Radio Science System, has been reported elsewhere[6].

### 3.1. Dual-Band Plasma Calibration

Any plasma along the ray path between the spacecraft and the DSN station produces a ray deflection and consequently a Doppler frequency shift. However, unlike the GRT effect, the plasma contribution to the signal is dispersive, proportional to the inverse square of the X- and Ka-Band frequencies, and it has opposite sign. The simultaneous X-Band Doppler data (7,175 MHz uplink, 8,425 MHz downlink) and Ka-Band Doppler data (34,316 MHz uplink, 32,028 MHz downlink) can be linearly combined to yield Doppler data which are significantly less noisy than either link alone, unless the ray path is close to conjunction where the technique fails.

The plasma noise is highly variable over all time scales, depending primarily on solar activity, in particular solar flares, coronal holes, and solar rotation. Because of stochastic plasma variability, the real assessment of how well the dual-band plasma correction works can be determined only by doing it. In fact it works very well for the SCE1 CL data. The algorithm for the corrections, in terms of the observed fractional frequency shifts at X-Band  $y_X$  and Ka-Band  $y_{Ka}$ , is[7]

$$y = 1.0575901y_{Ka} - 0.0575901y_X \quad (3)$$

where  $y$  designates the plasma-corrected fractional frequency shift. We multiply  $y$  by the downlink X-Band frequency on the data file ( $\sim 8,425$  MHz), and make a new file of X-Band data for further processing and analysis by the ODP.

### 3.2. Doppler Calibration for Earth's Troposphere

The Cassini radio signals are nondispersively refracted in the Earth's troposphere with a corresponding Doppler shift, a potential major error source for the SCE1 experiment. Tropospheric delay is a function of the spacecraft's elevation angle above the horizon, the altitude of the station above sea level, and

weather data on atmospheric pressure, temperature, and relative humidity. As the refractive properties of atmospheric gases behave differently from the water vapor, the tropospheric delay is partitioned into two components, the wet delay  $h_{wet}$  and the dry delay  $h_{dry}$ .

We use an ODP model based on weather data for purposes of removing a long-term trend ( $\sim 6$  hr) in the wet and dry components, and correct for short-term variations ( $\sim 30$  s) in the wet component by means of a stochastic component in the DSN's water-vapor radiometry data (AWVR) for path delay. It is not obvious that this scheme is anywhere near optimum, but indeed it does quite a good job in calibrating the plasma-calibrated data for the Earth's troposphere, the final step in our data processing before the data analysis phase. The tropospheric noise floor in fractional frequency of about  $4.2 \times 10^{-14}$  at 300 s sample interval is reduced to a floor of about  $2 \times 10^{-14}$  on average, and better than that between a region of 25 and 33 solar radii. Inside about 13 solar radii from the Sun's center, the plasma noise dominates the error budget, not the tropospheric noise.

The troposphere calibration also results in the loss of some points that are not obvious outliers at the plasma-calibration stage, or that are not improved by the AWVR data because of radiometer down time. The number of points on our data file after plasma calibration is 1697. After troposphere calibration, the number of points is reduced to 1575 points in 17 passes. A similar loss of points is claimed in the OL data processing[6], but there the final number of points is 1094 in 18 passes. We have retained about 52% more points in our CL analysis.

## 4. DATA ANALYSIS AND RESULTS

Our data processing is complete and we have generated a processed data file with 1575 Doppler points calibrated for plasma and the Earth's troposphere. The most straightforward analysis of this file involves weighting each pass of Doppler data by the inverse of the data variance for that pass, and letting the ODP estimate a set of parameters by nonlinear least squares with given starting values. This yields at least a local minimum for chi squared ( $\chi^2$ ). There are eight parameters in the fit, the Cartesian state for the spacecraft trajectory (Cartesian vector position and vector velocity for six parameters), a constant acceleration ATAR in the Spacecraft-Earth direction, and the PPN parameter  $\gamma$ . The initial conditions for the spacecraft trajectory are the heliocentric Cartesian position and velocity in Earth-equatorial coordinates of J2000 at epoch 6 June 2002 20:42:04.1848 ET, the barycentric coordinate time  $t$  used in the JPL ephemerides[4]. The parameter ATAR is included for purposes of correcting the ODP nongravitational model for the Cassini

Table I Eight Parameters, Data in Four Batches

Parameter	Estimate	Standard Error
$\Delta X$ (km)	-68.4	33.5
$\Delta Y$ (km)	-166.1	103.4
$\Delta Z$ (km)	-28.2	19.1
$\Delta \dot{X}$ (mm/s)	17.11	3.75
$\Delta \dot{Y}$ (mm/s)	-2.06	1.23
$\Delta \dot{Z}$ (mm/s)	-1.18	1.56
ATAR ( $10^{-13}$ km/s <sup>2</sup> )	-61.38	1.57
$\gamma - 1$ ( $10^{-5}$ )	-1.3	5.2
$\chi^2/(N-8)$	0.966	N = 1575

spacecraft, most notably solar radiation pressure and nonisotropic thermal emission produced by the spacecraft's power subsystem. For this basic fit,  $\chi^2$  is statistically 4.6% too large, which suggests the weighting of the data is a bit too optimistic. There are systematic signals in the Doppler residuals as well.

The best fit to the data is obtained by splitting it into batches and estimating ATAR as a stochastic parameter. The result for four batches is shown in Table I, with the errors adjusted to the best estimate of random error.

The spacecraft initial conditions or state vector are expressed as a correction to the state of the basic solution. In this fit,  $\chi^2/(N-8)$  is less than one, with  $N = 1575$ . No systematic signal is obvious in the residuals, unlike the basic fit. We adopt the batch-sequential fit as our final result for these proceedings. The result of the stochastic solution for ATAR is that the mean in Table I is correct for all the data interval, except for about nine days starting near conjunction on June 21 and ending on June 30, where the magnitude of ATAR decreases by  $0.26 \times 10^{-13}$  km/s<sup>2</sup>, only 0.42% of the total correction to the ODP model for nongravitational forces. It is reasonable that the real acceleration could change by this much over nine days. Alternatively, there could be a drift in the Doppler data for a few days after conjunction that is not removed by the plasma calibration so near the solar limb.

The residuals from the batch-sequential fit split naturally into symmetric pre and post conjunction residuals with almost identical descriptive noise statistics (see Fig. 1 and Fig. 2). This natural splitting does not correspond to the batch intervals for the fit. There is overlap. The batch-sequential fit eliminates systematic residuals, but not because of an overly restrictive limit on the time interval for each batch. The residuals closest to conjunction are plotted in Fig 3. These too would be symmetric about conjunction if the Ka transmitter at DSS25 had not failed for four scheduled passes just prior to conjunction. We deleted data from the first pass immediately after conjunction when the DSS25 Ka-Band transmitter recovered and

became operational again. Unfortunately, data within one day of conjunction are useless, even with the Ka-Band uplink. The units for the residuals in the plots are  $\mu\text{m/s}$ . They have been converted from Doppler residuals  $\Delta\nu$  in units of Hz for the processed X-Band Doppler data by the formula  $v_r = c\Delta\nu/2\nu$ , with  $\nu$  equal to the downlink frequency of 8,425 MHz and  $v_r$  the Doppler velocity.

The mean value of  $\gamma - 1$  is at minus  $0.25\sigma$ . If positive values of  $\gamma - 1$  are ruled out, the 95% confidence interval for  $\gamma - 1$  is between  $-2.14\sigma$  and zero. We conclude that in terms of the Brans-Dicke parameter  $\omega = (1 - 2\gamma)/(\gamma - 1)$ ,  $\omega > 9000$  with 95% confidence.

## Acknowledgments

We thank JPL's Radio Science Systems Group for making available the second round of AWVR processing and for many helpful discussions, especially Sami W. Asmar, Elias Barbunis and Gene L. Goltz. The Cassini Navigation Team (Jeremy B. Jones, Team Leader) provided helpful advice on the CL data. We also thank the Cassini Radio Science Team (Arvydas J. Kliore, Team Leader) for facilitating the SCE1 experiment, and the Cassini Project (Robert T. Mitchell, Project Manager) for agreeing in April 2001 to fully support SCE1. This work was sponsored by the Cassini Project and was performed at the Jet Propulsion Laboratory, California Institute of Technology, under contract with NASA.

## References

- [1] O. I. Yakolev, *Space Radio Science*, (Taylor and Francis, New York, 2002).
- [2] C. M. Will, *Theory and Experiment in Gravitational Physics, Rev. ed.*, (Cambridge University Press, Cambridge 1993).
- [3] I. I. Shapiro, "Fourth Test of General Relativity," *Phys. Rev. Lett.* **13**, 789-791 (1964).
- [4] T. D. Moyer, *Formulation for Observed and Computed Values of Deep Space Network Data Types for Navigation*, JPL Publication 00-7 (2000).
- [5] R. D. Reasenber, et al., "Viking Relativity Experiment: Verification of Signal Retardation by Solar Gravity," *Astrophys. Jour.* **234**, L219-L221 (1979).
- [6] B. Bertotti, L. Iess and P. Tortora, "A Test of General Relativity Using Radio Links with the Cassini Spacecraft," *Nature* **425**, 374-376 (2003).
- [7] B. Bertotti and G. Giampieri, "Solar Corona Plasma in Doppler Measurements," *Solar Phys.* **178**, 85-107 (1998).

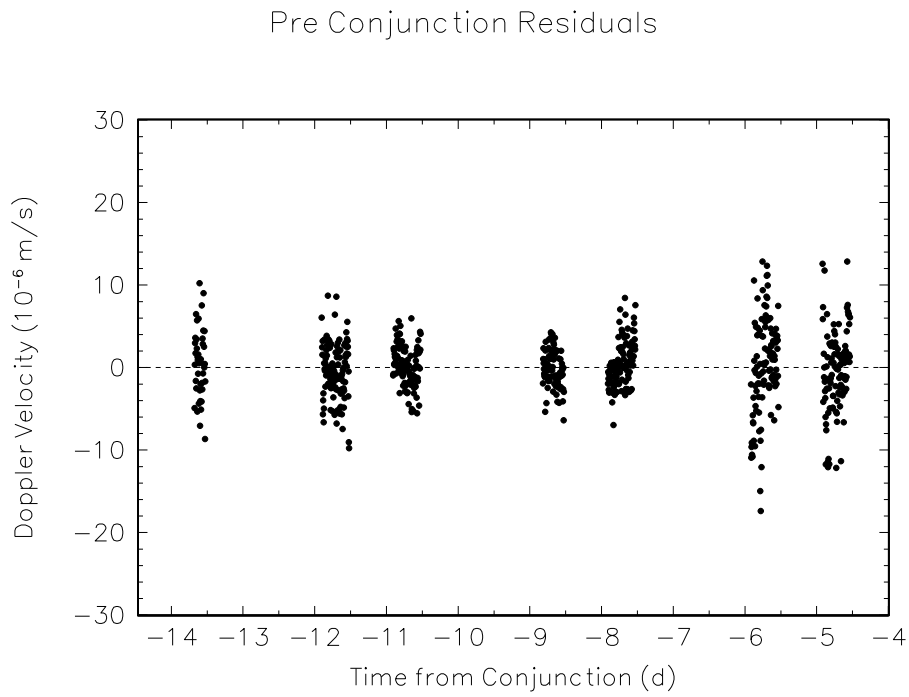


Figure 1: Plot of the pre conjunction residuals from the batch-sequential fit ( $N = 677$ ,  $\sigma = 3.95 \mu\text{m/s}$ ). The break between the first and second batch occurs at about - 8 d

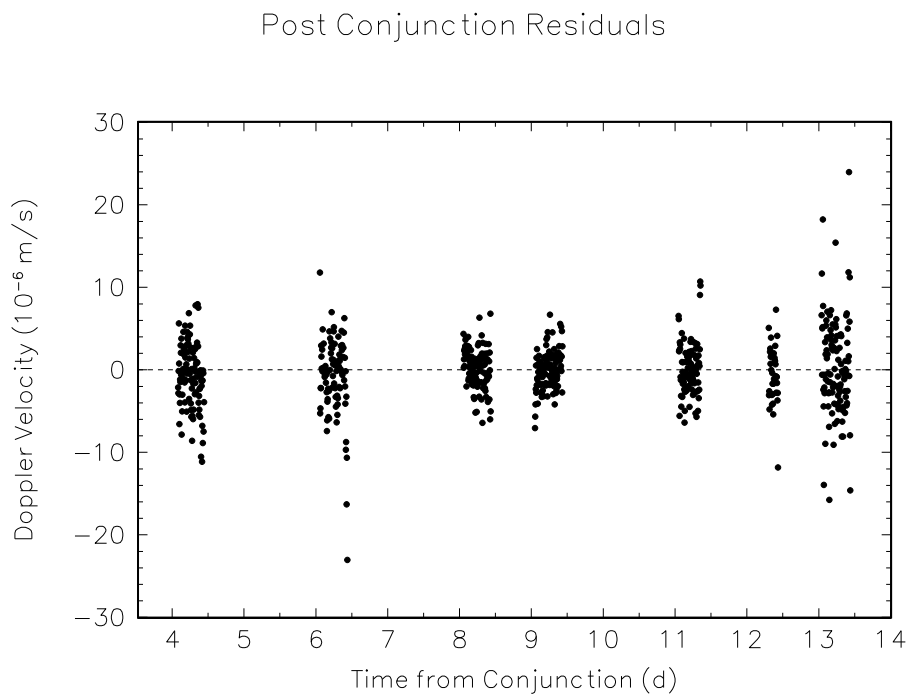


Figure 2: Plot of the post conjunction residuals from the batch-sequential fit ( $N = 652$ ,  $\sigma = 3.98 \mu\text{m/s}$ ). The break between the third and fourth batch occurs at about 8 d.

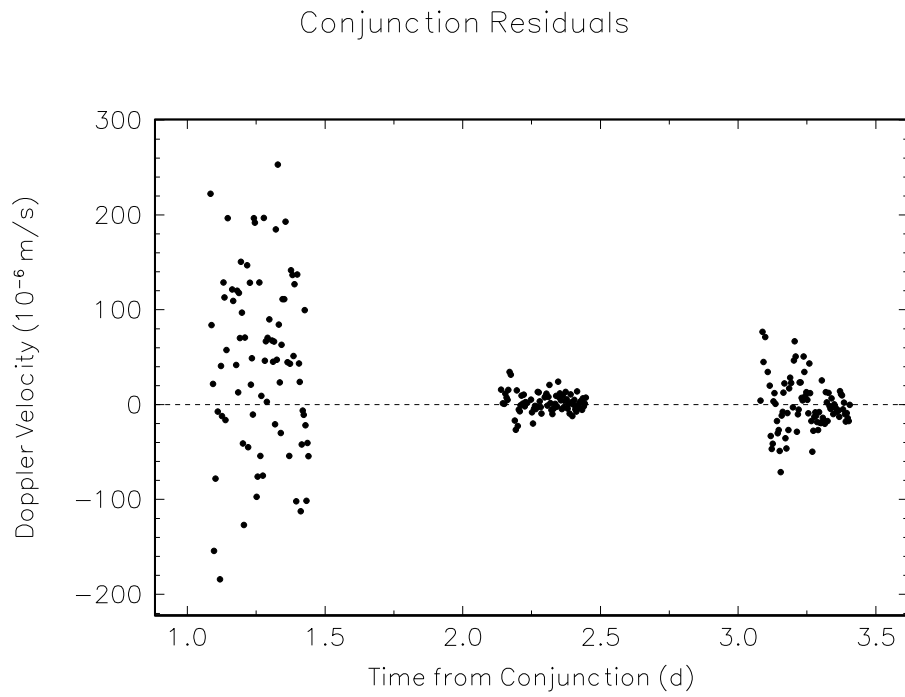


Figure 3: Plot of the residuals closest to conjunction from the batch-sequential fit ( $N = 246$ ). Note the change in scale from Fig. 1 and Fig. 2. The noise is not stationary. The break between the second and third batch occurs just prior to conjunction.